ELSEVIER

Surface Science 391 (1997) 134–144

surface science

The surface chemistry of propylene adsorbed on Mo(100), oxygen-covered Mo(100) and MoO_2

G. Wu, W.T. Tysoe *

Department of Chemistry and Laboratory for Surface Studies, University of Wisconsin–Milwaukee, Milwaukee, WI 53211, USA

Received 10 February 1997; accepted for publication 19 May 1997

Abstract

Propylene adsorbed on Mo(100) and oxygen-covered Mo(100) thermally decomposes to desorb hydrogen and deposit carbon, desorbs molecularly, self-hydrogenates forming propane, or decomposes to ultimately form adsorbed C_1 species, which hydrogenate to form methane. Since the hydrogen desorption yield decreases linearly with increasing oxygen coverage, it is proposed that propylene completely thermally decomposes on the four-fold hollow sites on Mo(100). Adsorbed propylene can self-hydrogenate to form propane and predosing the surface increases the propane yield indicating that it is formed by reaction of propylene with surface hydrogen. The activation energy for both of these processes increases with increasing oxygen coverage, a trend that is rationalized by proposing that propylene adsorbs on molybdenum by π donation to the surface. Finally, methane is formed in yields greater than found for ethylene on oxygen-covered Mo(100) and the methane yield increases with increasing oxygen coverage up to 0.67 monolayers and decreases at higher coverages. No other hydrocarbons are detected following propylene adsorption on any oxygen-covered surface and it is suggested that an initial carbon–carbon bond cleavage leads to the ultimate formation of methane by reaction of C_1 species with adsorbed hydrogen. © 1997 Elsevier Science B.V.

Keywords: Chemisorption; Low index single crystal surfaces; Molybdenum; Propylene; Soft X-ray photoelectron spectroscopy; Thermal desorption spectroscopy

1. Introduction

It has been shown previously that ethylene can undergo a variety of reactions on oxygen-modified Mo(100) including hydrogenation, decomposition into carbon and hydrogen and also dissociation to form surface C_1 species which then hydrogenate to form methane [1–3]. Such carbene formation has been suggested to be the first step in the carbene–metallacycle mechanism proposed for both homogeneous and heterogeneous olefin metathesis [4–12]. It has also been demonstrated that C_1 species formed from ethylene can polymerize on metallic molybdenum to form higher molecular weight hydrocarbons [13–15]. This paper extends this work to the examination of propylene, the simplest olefin for which metathesis is nondegenerate. In this case, metallic molybdenum [16] and molybdenum oxides [17] all catalyze metathesis (i.e. ethylene and butene formation) at relatively high temperatures, but with rather low selectivity. As noted above, this reaction probably proceeds by carbene polymerization. Another reaction route, which has a much lower activation energy (6 versus 60 kcal/mol), is found at lower temperatures (below 650 K), in particular on MoO_2

* Corresponding author. Fax: (+1) 414 229.5530; e-mail: wtt@alpha2.csd.uwm.edu

PII S0039-6028(97)00472-X

model oxide catalysts. We have therefore also studied the chemistry of propylene on MoO_2 films. As was found for ethylene adsorption on this surface [1], propylene is essentially unreactive on MoO_2 under ultra-high vacuum (UHV) conditions since propylene adsorbs and desorbs molecularly.

Oxygen overlayers also affect the catalytic activity of molybdenum where the addition of ~ 0.6 monolayers of oxygen (where a monolayer is referenced to the number of unit cells on the (100) surface) leads to the maximum enhancement [13]. The chemistry of propylene is also studied on these surfaces. As noted above, methane is formed from ethylene on oxygen-modified Mo(100) where methylenes formed by direct carbon–carbon bond scission react with hydrogen to form methane [1]. The presence of more labile methyl groups in propylene open up the possibility that carbenes could be formed by other routes. These alternatives will be explored in the following.

2. Experimental

Two pieces of equipment were used for these experiments; both have been described in detail elsewhere [18,19]. Briefly, the first consists of an ion- and sublimation-pumped, bakeable UHV chamber operating at a base pressure of $< 1 \times 10^{-10}$ torr following bakeout. The Mo(100) sample is mounted to the end of a rotatable manipulator by means of 0.5 mm diameter tantalum heating wires spot-welded to 2 mm diameter tantalum rods. In addition, the manipulator has been retrofitted with electron-beam heating [19]. This allows the sample to be repeatedly heated to > 2000 K without any adverse effects on the heating wires. The sample could also be cooled to ~ 80 K via thermal contact to a liquid-nitrogen filled reservoir. Resistive heating was used to collect temperature-programmed desorption (TPD) data. These were collected using a computer-multiplexed quadrupole mass spectrometer that could record up to five masses sequentially using a heating rate of 10 K/s. The analyzer head of the quadrupole was enclosed in an evacuated shroud with a 1 cm diameter hole in the front to minimize signals not arising from the sample entering the mass spectrometer ionizer.

The chamber was also equipped with a four-grid retarding field analyzer (RFA) which was used to obtain LEED images of the sample and to collect Auger data. The sample was cleaned by heating in $\sim 2.5 \times 10^{-7}$ torr of oxygen at 1200 K for 5 min to remove carbon and then rapidly heating in vacuo to 2100 K to remove oxygen. This resulted in the diffusion of further carbon to the surface and this procedure was repeated until no impurities, particularly carbon, were noted on the surface after heating to 2100 K.

Ultraviolet photoelectron spectra were obtained at the Wisconsin Synchrotron Radiation Center using the Aladdin storage ring. The stainless-steel UHV chamber used for these experiments operated at a base pressure of $\sim 1 \times 10^{-10}$ torr following bakeout and was attached to the end of a Mark V Grasshopper monochromator. The chamber was equipped with a quadrupole mass analyzer for residual gas analysis and to test gas purities. It was also equipped with a double-pass, cylindrical-mirror analyzer which was used to collect both Auger and photoelectron spectra. Auger spectra were excited using a 3 keV electron beam and collected by counting the scattered electrons and the $dn(E)/dE$ Auger spectrum obtained by numerically differentiating the $n(E)$ signal. The analyzer was operated at a pass energy of 25 eV to collect photoelectron spectra and this yielded an overall spectral resolution of 0.15 eV. These were excited using 60 eV radiation which has been shown previously to yield the optimum C 2s to background intensity ratio on Mo(100) [20].

The propylene (Aldrich, WI, 99.9% purity) was transferred to a glass bottle and further purified by repeated bulb-to-bulb distillations and stored in glass until use. The oxygen (AGA Gas, Inc., OH, 99%) was transferred from the cylinder to a glass bulb and also redistilled.

Oxygen overlayers were prepared by saturating the Mo(100) surface (20 L O_2 exposure at 1050 K; 1 L $= 1 \times 10^{-6}$ torr s) and annealing to various temperatures to remove oxygen to obtain the requisite coverage. The adsorption of oxygen on Mo(100) has been studied very extensively [21–24] and the oxygen coverages were reproduced from their char-

acteristic LEED patterns and confirmed from their relative O/Mo Auger ratios (by monitoring the O KLL and Mo LMM Auger transitions). MoO_2 films were grown using a literature protocol [25] where metallic molybdenum was oxidized using 3×10^{-5} torr of oxygen for 120 s with the sample heated to 1050 K.

3. Results

Various oxygen overlayers of different coverages were obtained by annealing an oxygen-saturated p(1 × 1) surface to various temperatures and have been carefully documented [21–24]. MoO_2 is synthesized as described above. The relative oxygen coverages were checked by measuring the O:Mo Auger ratio as a function of annealing temperature. Note that MoO_2 provides a model catalyst that mimics the metathesis activity of high loadings of molybdenum oxide supported on alumina and the metathesis activity of metallic molybdenum modified by oxygen overlayers has been shown to increase as a function of oxygen coverage from θ_O–0 ML (clean surface) to $\theta_O = 0.6$ ML and decrease thereafter [13].

Fig. 1 shows the photoelectron spectrum of propylene adsorbed on MoO_2 displaying the C and O 2s region up to 27 eV binding energy (*BE*) following a 10 L exposure. The annealing temperature is displayed adjacent to each spectrum and a spectrum of MoO_2 prior to adsorption of propylene is shown for comparison and is indicated as "clean". The intense peak at 22.5 ± 0.2 eV is assigned to emission from the O 2s orbital and the broad structure between 5 and 10 eV binding energy is due to emission from O 2p orbitals. Features below ~3 eV *BE* are due to emission of molybdenum d electrons. Additional peaks are evident at 12.5 ± 0.2, 16.0 ± 0.2 and at 17.6 ± 0.2 eV binding energy (*BE*) and are assigned to emission from the molecular orbitals constructed from linear combinations of 2s orbitals of propylene. Note that the photon energy was selected to enhance the intensity of these levels. The vertical lines below these spectra are the peak positions in the gas-phase photoelectron spectrum of propylene [26] and agree well with the 2s-derived levels. Note

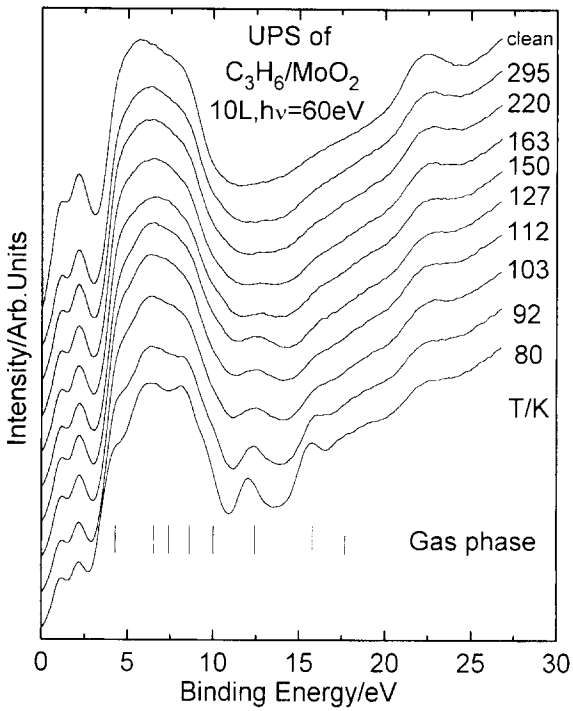

Fig. 1. Ultraviolet photoelectron spectra displaying the carbon and oxygen 2s region obtained following propylene adsorption (10 L) on an MoO_2 surface as a function of sample annealing temperature. The annealing temperature is displayed adjacent to the corresponding spectrum. These spectra were excited using 60 eV photons.

also that the structure superimposed on the broad O 2p peak between 5 and 10 eV binding energy correlates with the expected peak positions for propylene. As the sample temperature increases, the intensities of the 2s-derived peaks decrease so that, after the sample has been annealed to ~220 K, these features are essentially completely absent leaving only oxygen photoemission features. The corresponding temperature-programmed desorption spectra, obtained at various masses by exposing a MoO_2 sample to propylene (5 L exposure) at 80 K and collecting the spectrum at a heating rate of 10 K/s, are displayed in Fig. 2. The sharp feature at ~160 K is assigned to a condensed propylene multilayer since it continues to grow with increasing propylene exposure without saturation. The broader feature at ~260 K is due to an adsorbed propylene layer. These results indicate that propylene merely adsorbs and desorbs

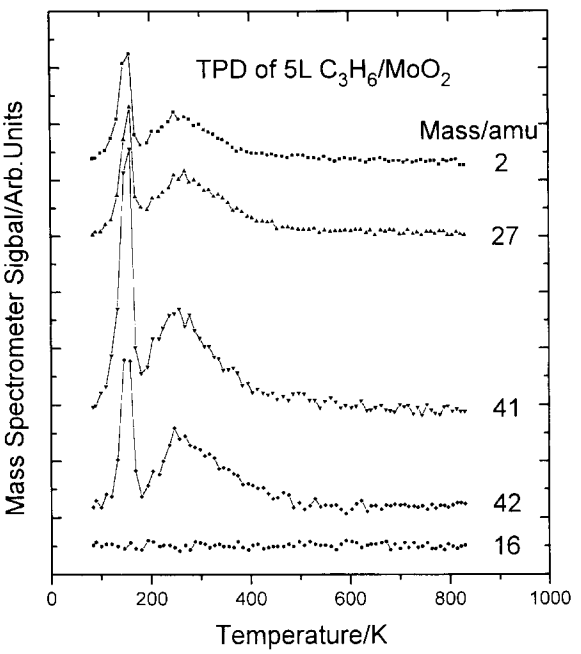

Fig. 2. Temperature-programmed desorption spectra collected at several masses following exposure of MoO_2 to 5 L of propylene. The masses monitored are displayed adjacent to the corresponding spectrum.

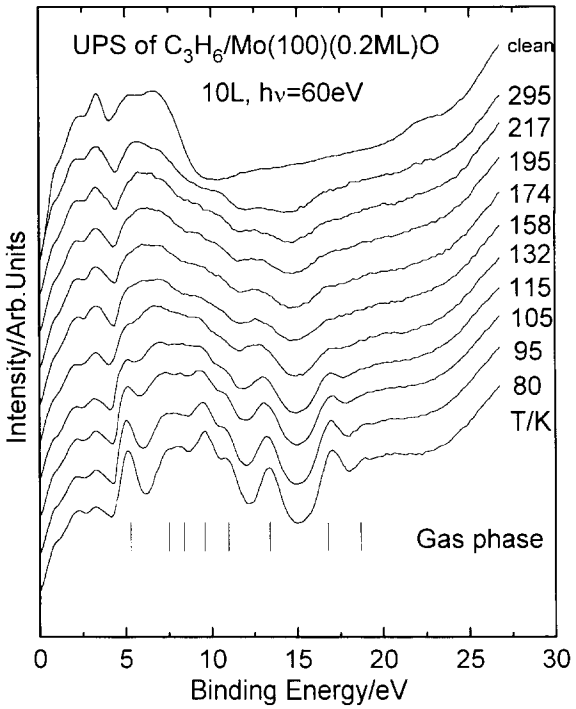

Fig. 3. Ultraviolet photoelectron spectra displaying the carbon and oxygen 2s region obtained following propylene adsorption (10 L) on a Mo(100) surface covered with 0.2 monolayers of oxygen as a function of sample annealing temperature. The annealing temperature is displayed adjacent to the corresponding spectrum. These spectra were excited using 60 eV photons.

molecularly on MoO_2 in a behavior exactly identical to that found for ethylene [1]. A simple Redhead analysis of this 260 K desorption state using a typical pre-exponential factor of 1×10^{13}/s and the experimental heating rate of 10 K/s yields a desorption activation energy of ~14.7 kcal/mol, slightly higher than the corresponding value for ethylene of ~11.6 kcal/mol [1]. Thus, although MoO_2 provides a model catalyst that mimics the metathesis activity of a supported oxide under high-pressure conditions, again it appears to be chemically extremely inert in ultrahigh vacuum.

Fig. 3 shows the photoelectron spectra of propylene adsorbed on oxygen-covered Mo(100) after annealing to various temperatures where the oxygen coverage is 0.2 monolayers and the spectrum of an oxygen-covered surface prior to exposure to propylene is shown for comparison (again designated as "clean"). Annealing temperatures are displayed adjacent to their corresponding spectra. Again the molecular 2s-derived energy levels are evident between 12 and 20 eV binding energy indicating that propylene adsorbs molecularly. The positions of the features agree reasonably with those for gas-phase propylene [26] although the peak spacing in the adsorbate may be slightly larger than in the gas-phase molecule indicative of some molecular distortion for the adsorbed propylene. A similar effect was observed for ethylene on oxygen-covered Mo(100) [1]. The agreement between the features seen between 5 and 12 eV (assigned to orbitals arising from atomic 2p orbitals) and gas-phase propylene is also quite good. As the sample temperature is raised, these features attenuate. Note that the highest binding energy 2s emission feature at ~17.5 eV bonding energy attenuates preferentially and the spacing between the remaining features increases indicative of surface decomposition of the propylene. There also appears to be an enhanced growth in the peak

at ~12 eV *BE* indicative of the formation of adsorbed C_1 species. A similar situation is found with the addition of ~0.8 monolayers of oxygen where propylene apparently adsorbs intact at ~80 K, although the saturation coverage is clearly lower in this case due to the presence of larger amounts of oxygen. In this case, the 2s peak positions for adsorbed propylene are closer to the gas-phase values suggesting that the molecule is only slightly distorted on adsorption. As the sample is heated, these peaks attenuate and are replaced after annealing to ~200 K by a single feature at ~12 eV binding energy, again suggesting that the propylene decomposes on this surface, finally yielding adsorbed C_1 species. For a surface covered with 1.35 monolayers of oxygen, propylene adsorbs at low temperature but the majority of the adsorbed species appears to desorb molecularly since all of the propylene-induced features decrease in intensity simultaneously.

The hydrogen (2 amu) desorption spectra for various oxygen-covered surfaces are displayed in Fig. 4. Clean Mo(100) exhibits three main features at ~230 and 380 K with an additional peak at a rather high temperature of ~580 K. The lower temperature structure is similar to that found for ethylene on metallic Mo(100), but no 580 K peak was detected in this case. This feature disappears following the addition of 0.2 monolayers of oxygen. The 250 and 380 K peaks shift to higher temperatures as the oxygen coverage increases eventually leading to a small and broad peak centered at ~500 K at an oxygen coverage of 0.95 monolayers.

The corresponding propylene (41 amu) temperature-programmed desorption spectra are displayed in Fig. 5. There is a broad similarity between the chemistry of propylene on oxygen-covered Mo(100) and that of ethylene on the same surfaces. The propylene yield from metallic molybdenum is rather small and increases with the addition of oxygen reaching a maximum at ~1 ML and decreasing thereafter. Propylene desorbs from clean Mo(100) in two states centered at ~190 and ~350 K. The 190 K state increases in temperature slightly to 220 K when co-adsorbed with 0.67 monolayers of oxygen. The ~350 K peak maintains an approximately constant peak position and a peak starts to grow at ~280 K at a coverage of 0.67 and increases in intensity at $\theta(O)=0.83$ and 0.95 and decreases slightly at the oxygen monolayer and is completely absent above this coverage. The corresponding oxygen LEED patterns are displayed on this figure and the presence of this 280 K state is associated with the appearance of the $\sqrt{5}\times\sqrt{5}R26°33'$ LEED structure. It has been suggested that the surface reconstructs while forming this structure so that the peak in this case may be associated with a reconstructured surface. A similar effect has been noted for ethylene adsorbed on oxygen-covered Mo(100). At higher coverages, the 220 K peak (present at 190 K on the clean surface) further shifts to ~280 K with an oxygen coverage of 1.5 ML. This effect has been noted previously and explained by assuming that alkenes adsorb via donation of π electrons to vacant d-orbitals in the substrate. This is enhanced by the addition of oxygen which effectively lowers the Fermi energy and results in a larger heat of adsorption [3,27,28].

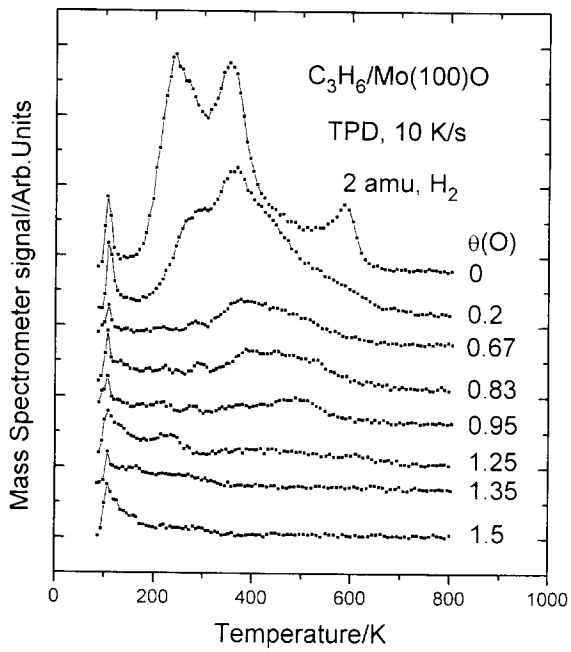

Fig. 4. Hydrogen (2 amu) temperature-programmed desorption spectra collected after saturating various oxygen-covered surfaces of Mo(100) with propylene. The oxygen coverages are displayed adjacent to the corresponding spectrum.

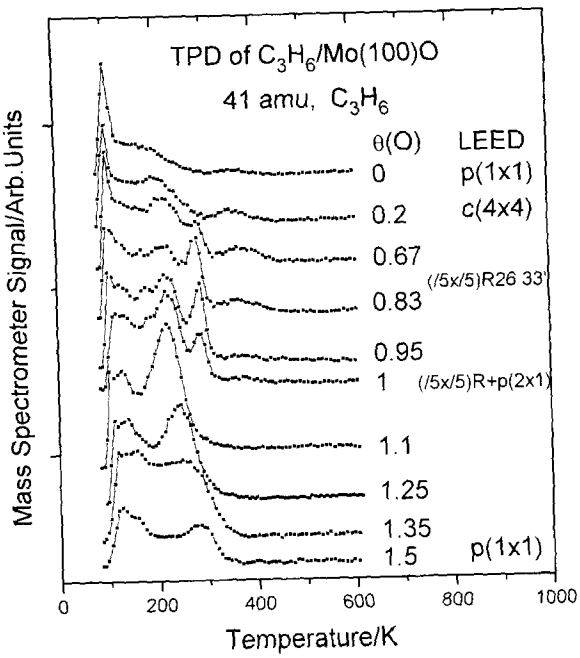

Fig. 5. Propylene (41 amu) temperature-programmed desorption spectra collected after saturating various oxygen-covered surfaces of Mo(100) with propylene. The oxygen coverages and their LEED patterns are displayed adjacent to the corresponding spectrum.

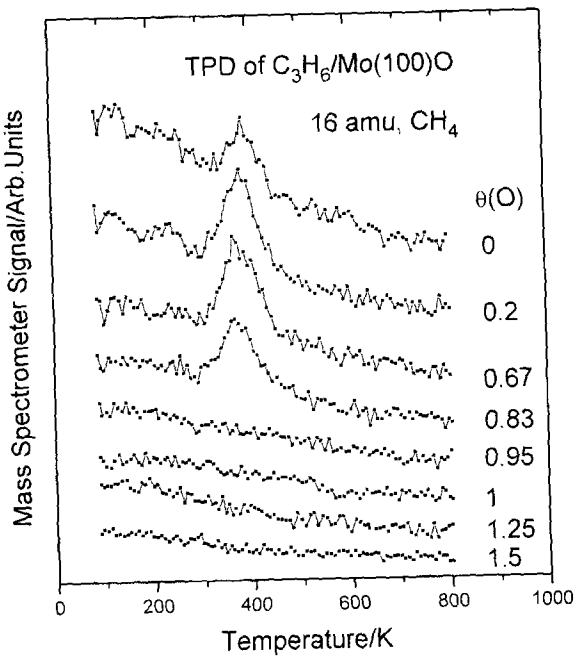

Fig. 6. Methane (16 amu) temperature-programmed desorption spectra collected after saturating various oxygen-covered surfaces of Mo(100) with propylene. The oxygen coverages are displayed adjacent to the corresponding spectrum.

Methane was also found to desorb from some of the oxygen-covered surfaces. These results are illustrated in Fig. 6 which displays the methane (16 amu) desorption spectra obtained after saturating various oxygen-covered Mo(100) surfaces with propylene. The desorption of methane was confirmed by comparing the desorption intensity with the mass spectrometer ionizer fragmentation pattern for methane. Methane desorbs at slightly below 400 K where the yield varies with oxygen coverage. Somewhat similar results were found for ethylene on oxygen-covered Mo(100) where methane was found to desorb at ~370 K [1]. In this case, however, the methane yield as a function of oxygen coverage was different. First, the *total* methane yield at any coverage is much larger than that for ethylene. Second, no methane was found to desorb from metallic molybdenum when ethylene was adsorbed whereas there is a significant methane yield from propylene on clean Mo(100). The methane yield increases slightly as the oxygen coverage increases reaching a maximum at $\theta(O) = 0.67$ (which was also the case for ethylene adsorption) and then decreases at higher coverages. No methane is found to desorb from surface coverages greater than 1 monolayer of oxygen. Methane formation has been found previously due to methylene hydrogenation both on O–Mo(100) [19] and on Mo(110) [29] by grafting methylene species on the surface by decomposing methylene iodide. It has been demonstrated that the rate-limiting step on O–Mo(100) is the final hydrogenation of an adsorbed methyl group to methane [30]. It is interesting also to note that methyl radicals adsorbed directly on Mo(100)+1.0 monolayer of oxygen desorb as methane at ~450 K [31], slightly higher in temperature than found here. Hydrogen due to methyl group decomposition also desorbs at ~500 K from this surface, close to the hydrogen desorption peak position seen following propylene adsorption on a surface covered by 0.95 monolayers of oxygen (Fig. 4) although no methane is found in this case. In the case of CH_x

species formed from iodine-containing precursors, methane was found to form at much lower temperatures (~250 K). The origin of these differences is not entirely clear although, since the hydrogenation kinetics of methyls formed from methyl iodide [30] and methyl radicals [31] are very different, this implies that adsorbed iodine strongly affects the methane formation temperature. Intriguingly, the methane desorption kinetics are apparently only slightly affected by oxygen when formed from propylene (Fig. 6).

Self-hydrogenation of propylene to form propane is also found on molybdenum and oxygen-covered molybdenum. It has been shown previously that metallic molybdenum can catalyze ethylene hydrogenation [16]. The temperature-programmed desorption spectrum of propane formed by propylene adsorption on Mo(100) is shown in Fig. 7 (by monitoring the 29 amu peak) and reveals a single feature centered at 190 K, slightly lower in temperature than ethane self-hydrogenation on Mo(100). The peak temperature increases to ~220 K as the oxygen coverage increases with a corresponding decrease in yield so that for $\theta(O)=0.83$, essentially no propane is formed. Note that the increase in desorption activation energy is in accord with the increase in propylene adsorption energy noted above as a function of oxygen coverage. The effect of predosing the clean Mo(100) surface with hydrogen is also shown in Fig. 8 where the propane yield increases and the peak temperature decreases with the addition of hydrogen to the surface where a measurable effect is noted with the addition of even a very small amount of hydrogen (0.05 L). These results indicate that adsorbed propylene reacts with adsorbed hydrogen to form propane.

Finally, no other desorbing species, for example, oxygen-containing molecules or water, were found to desorb from any of the oxygen-covered surfaces. In addition, no C_2 compounds, such as ethylene or ethane were detected following propylene adsorption on any of the surfaces investigated.

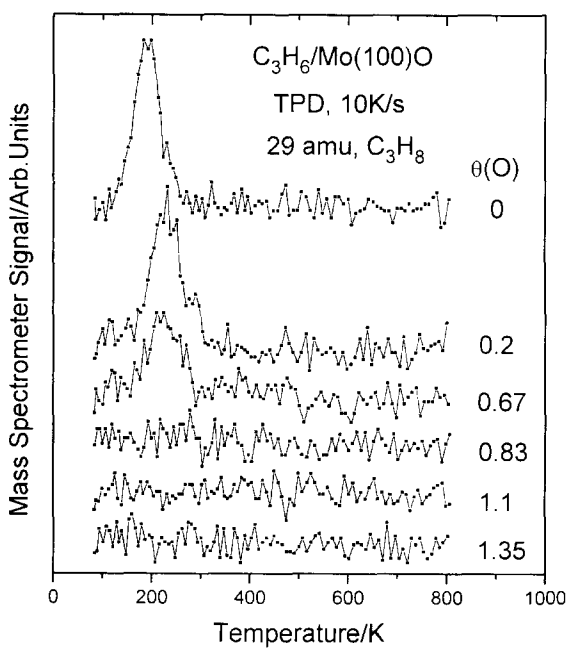

Fig. 7. Propane (29 amu) temperature-programmed desorption spectra collected after saturating various oxygen-covered surfaces of Mo(100) with propylene. The oxygen coverages are displayed adjacent to the corresponding spectrum.

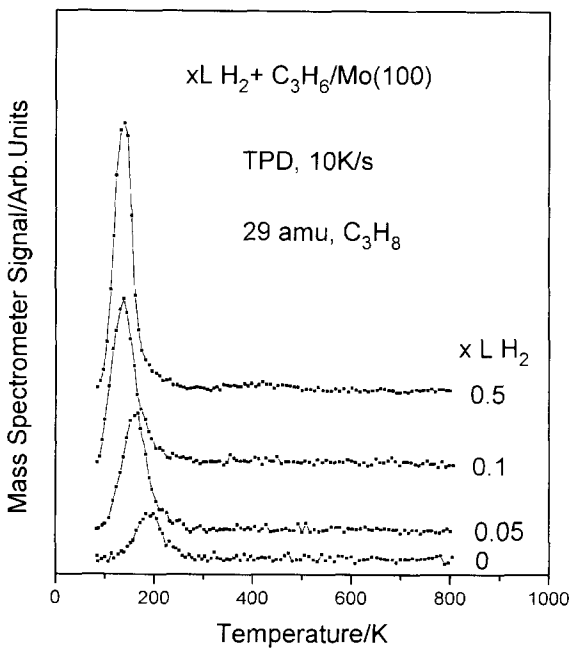

Fig. 8. Propane (29 amu) temperature-programmed desorption spectra obtained following various exposures of a Mo(100) surface to hydrogen and then saturating the surface with propylene. Hydrogen exposures are displayed adjacent to the corresponding spectrum.

4. Discussion

The reaction pathways for propylene on oxygen-covered Mo(100) can be summarized as:

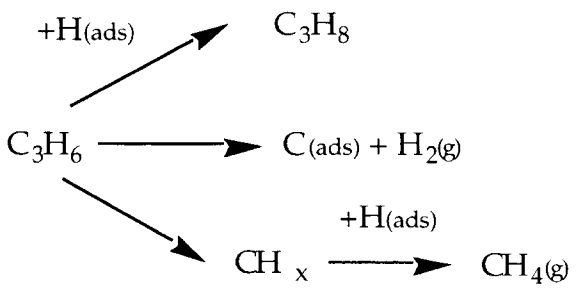

Hydrogen (Fig. 4) is the major desorption product found following adsorption of propylene on Mo(100) and oxygen-covered Mo(100) resulting from a total thermal decomposition of adsorbed propylene to form carbon and hydrogen. Fig. 9 shows a plot of the total hydrogen yield from a propylene-saturated surface (obtained by integrating the 2 amu TPD data of Fig. 4) as a function of oxygen coverage. The graph decreases approximately linearly with increasing oxygen coverage implying that the sites at which propylene decomposes are being directly blocked by oxygen. Note that propylene adsorbed on MoO_2 yields essentially no hydrogen in accord with this trend (Fig. 2). A similar effect has been seen for ethylene on oxygen-covered Mo(100) [1] and, since oxygen adsorbs at the four-fold hollow sites, it is proposed that both ethylene and propylene thermally decomposes to form carbon and hydrogen on these sites.

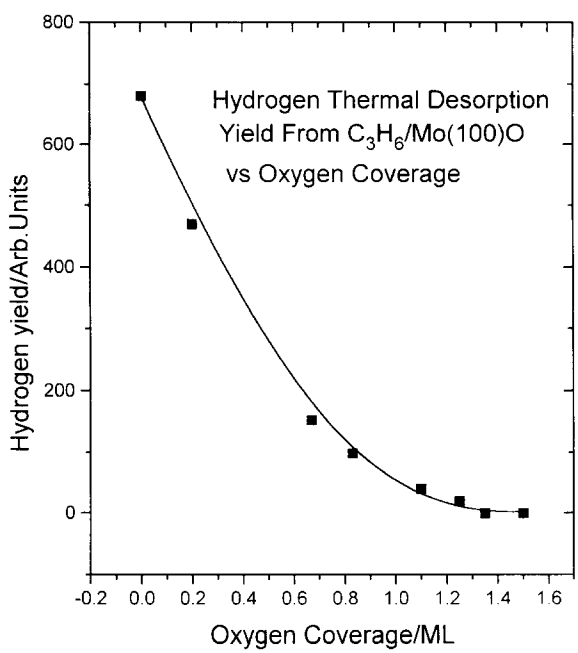

Fig. 9. Plot of the total hydrogen thermal desorption yield from propylene adsorbed onto oxygen-covered Mo(100) as a function of oxygen coverage.

Photoelectron spectroscopy (for example, Fig. 3) indicates that propylene adsorbs molecularly at liquid nitrogen temperatures on these surfaces and thermally decomposes on heating ultimately forming C_1 species. It is also important to note that no C_2 compounds are found to desorb from any of these surfaces. The peak position for the formation of methane is essentially identical irrespective of whether it is formed from ethylene or propylene, indicating that the rate-limiting methane-formation step is the same in both cases. In the case of homogeneous metathesis catalysis, the formation of an active system requires the participation of a co-catalyst, often a metal alkyl [32,33]. However, the heterogeneous reaction is generally carried out in the absence of a co-catalyst. In this case, several carbene formation routes have been proposed. In the first, partial hydrogenation of an adsorbed alkene to form an alkyl group is suggested [34]. In the case of propylene, this would result in the formation of an adsorbed propyl group if a terminal carbon were hydrogenated and an isopropyl group for hydrogenation at the 2-position. Carbenes are suggested to form by subsequent α-hydride elimination [34]. This carbene formation pathway would, of course, not give rise to methane. Note that the data in Figs. 7 and 8 indicate that propylene can hydrogenate to form propane which necessarily must involve the formation of the half-hydrogenated (alkyl) state. Presumably, in this case, any subsequent hydrogenation to form propane is much faster than the rate of α-hydride elimination. In any case, β-hydride elimination has been shown to be favored on transition metal surfaces in other cases [35]. In addition, no H–D exchange was detected for ethylene co-adsorbed with deuterium

on O–Mo(100) as would be expected for a reaction involving an initial hydrogenation step and subsequent rapid β-hydride elimination. Another mechanism proposed by Green [36,37] involves the initial formation of a π-allylic intermediate via hydrogen abstraction from the methyl group. Note that, based on the relative C–H bond strengths ($H–CH_2$, 111 kcal/mol versus H–allyl of 89 kcal/mol, [38]), this is likely to be a rather favored initial pathway. The resulting allylic species is then proposed to hydrogenate at the β-position forming a metallacycle. This is proposed to decompose in exactly the same manner as in the conventional carbene–metallacycle pathway to produce an alkene leaving behind the carbene [4–12] which, in this case, would evolve ethylene and deposit a methylene (CH_2) species. Note, however, that no ethylene is found to desorb from the surface as required by this pathway. In addition, preliminary experiments have been carried out in which allylic species have been grafted to the surface by thermally decomposing $CH_2I–CH=CH_2$ on the oxygen-covered Mo(100). This merely thermally decomposes to yield hydrogen in the absence of pre-adsorbed hydrogen. When $CH_2I–CH=CH_2$ is adsorbed on a hydrogen pre-covered surface, the reaction is primarily at the α-position and neither ethylene nor methane are detected. In addition, this carbene formation pathway does not apply to ethylene since it has no alkyl groups while carbene formation is also found in that case. Certainly, in the latter case, carbene formation appears to proceed via a direct carbon–carbon bond scission, and one of the roles played by adsorbed oxygen in that case is to promote that reaction [1]. An analogous reaction for propylene would lead directly to carbene (CH_2) and methyl carbene ($CH_3–CH$) formation. Preliminary experiments to graft a methyl carbene onto the surface by thermally decomposing 1,1 diiodoethane reveal that this can react to form methane although the decomposition pathway in this case is unclear. This chemistry is currently being investigated in greater detail.

It is also found that the methane yield is affected by the presence of oxygen so that the yield increases up to an oxygen coverage of $\sim$0.67 monolayers and decreases thereafter. There is a slight decrease in peak desorption temperature as the oxygen coverage increases. As noted above, methyl species grafted onto Mo(100) pre-covered by a monolayer of oxygen desorb as methane at 450 K, while methyl and methylene species formed from iodine-containing molecules desorb at lower temperatures ($\sim$250 K). Methyl and methylene species adsorb predominantly by electrons from the substrate d-orbitals filling vacant 2p-derived levels on the carbon so that the adsorbed C_1 species will be negatively charged [1]. The addition of oxygen will destabilize the adsorbed carbene and facilitate hydrogenation. This may contribute to the shift in methane desorption peak temperature evident in Fig. 6. However, this would predict that methane should form at even *lower* temperatures on a surface covered by 1.0 monolayers of oxygen. However, as illustrated by Fig. 9, the inventory of adsorbed hydrogen is decreasing with increasing coverage and, as illustrated by the data of Fig. 8, small changes in hydrogen coverage can substantially alter the peak positions of hydrogenation products. The relatively modest shift in peak position seen in Fig. 6 may be the nett result of these two effects, one an electronic effect (decreasing the desorption temperature) and a hydrogen availability effect (increasing the desorption temperature). This does not rationalize the extremely large effect that iodine has on lowering the methane desorption temperature to $\sim$250 K. This may be rationalized by differences in ionic radii of iodine (2.2 Å) and oxygen (1.32 Å) [38] compared with the Mo–Mo spacing on the (100) surface (4.16 Å [39]). There are several effects which might change the methane yield. First, the C=C dissociation probability is promoted by the addition of oxygen [1,3,27]; and second, carbene dehydrogenation to yield adsorbed carbon and to evolve hydrogen competes with hydrogenation to methane. The carbene thermal decomposition temperature increases with the addition of oxygen [19] leading to a corresponding increase in the methane formation probability as the oxygen coverage increases. It is interesting to note that the 350 K hydrogen desorption feature that increases in peak temperature as the oxygen coverage increases (Fig. 4) is at the temperature at which carbenes grafted onto oxygen-covered Mo(100) by methylene iodide

decomposition thermally decompose to yield hydrogen [19] so that this peak may be due to this process.

As the oxygen coverage increases further above 0.67, the methane yield decreases once again. This result is probably partly due to the lack of available hydrogen obtained from propylene dehydrogenation on the surface since the number of available four-fold sites decreases (Fig. 9). Note that this general trend is similar to that for ethylene adsorbed on O–Mo(100) [1] except that the total yield for propylene is greater than that for ethylene. Further evidence for these effects comes from the data of Fig. 7, which show the variation in propane yield due to the self-hydrogenation of adsorbed propylene where the hydrogen derives from propylene that decomposes on the surface. The data in Fig. 8 emphasize that, in this case, the hydrogen required to form propane derives from the molybdenum surface since the propane desorption spectrum is significantly altered by pre-dosing hydrogen. In this case, the peak temperature decreases with increasing hydrogen exposure clearly indicative of a second-order reaction between adsorbed hydrogen and propylene.

5. Conclusions

Propylene reacts on Mo(100) and oxygen-covered Mo(100) in a manner very similar to that found for ethylene where it can thermally decompose to yield hydrogen, hydrogenate to form propane, dissociate and hydrogenate to give methane or desorb. All of these reactions are affected by the presence of oxygen on the surface. The total thermal decomposition, as indicated by the yield of hydrogen as a function of oxygen coverage, appears to take place at the four-fold hollow sites on the (100) which are blocked by oxygen thus preventing thermal decomposition. The methane yield varies strongly with oxygen coverage so that some methane is formed on the clean surface. The yield increases with increasing oxygen coverage to reach a maximum at $\theta_O = 0.67$ and decreases at higher coverages. This variation in methane yield is associated with an increase in the stability of the carbene and possibly an enhancement in the activity of the surface by the addition of oxygen. The yield decreases at higher coverage because of a lack of surface hydrogen.

The activation energy for propylene desorption is found to increase with increasing oxygen coverage. This effect has been noted previously and rationalized by suggesting that propylene adsorbs on molybdenum by donation of its π electrons into the vacant substrate orbitals of molybdenum. This behavior is generally the same as found for ethylene on oxygen-modified molybdenum.

Acknowledgements

We gratefully acknowledge support of this work by the US Department of Energy, Division of Chemical Sciences, Office of Basic Energy Sciences, under grant no. DE-FG02-92ER14289. This work is based upon research conducted at the Synchrotron Radiation Center, University of Wisconsin–Madison, which is supported by the NSF under award no. DMR-95-31009.

References

[1] G. Wu, B. Bartlett, W.T. Tysoe, Surf. Sci. (in press).
[2] L. Wang, W.T. Tysoe, Surf. Sci. 236 (1990) 325.
[3] J.E. Deffeyes, A.H. Smith, P.C. Stair, Surf. Sci. 163 (1985) 79.
[4] J.L. Hèrison, Y. Chauvin, Makromol. Chem. 141 (1970) 161.
[5] R.J. Haines, G.J. Leigh, Chem. Soc. Rev. 4 (1970) 161.
[6] E.O. Fischer, K.H. Dotz, Chem. Ber. 105 (1972) 3966.
[7] R.R. Schrock, J. Am. Chem. Soc. 98 (1976) 5399.
[8] R.H. Grubbs, D.D. Carr, C. Hoppin, P.C. Burk, J. Am. Chem. Soc. 98 (1976) 3478.
[9] J.J. Katz, J. Rothschild, J. Am. Chem. Soc. 98 (1976) 2519.
[10] C.P. Casey, H. Tuinstra, M.C. Saeman, J. Am. Chem. Soc. 98 (1976) 608.
[11] F.N. Tebbe, G.W. Parshall, D.W. Ovenall, J. Am. Chem. Soc. 101 (1979) 5074.
[12] T.R. Howard, J.B. Lee, R.H. Grubbs, J. Am. Chem. Soc. 102 (1980) 6878.
[13] B. Bartlett, C. Soto, R. Wu, W.T. Tysoe, Catal. Lett. 21 (1993) 1.
[14] B. Bartlett, H. Molero, W.T. Tysoe, Catal. Lett. (submitted).
[15] B. Bartlett, V.L. Schneerson, W.T. Tysoe, Catal. Lett. 3 (1995) 1.
[16] L. Wang, W.T. Tysoe, J. Catal. 128 (1991) 320.

[17] B.F. Bartlett, H. Molero, W.T. Tysoe, J. Catal. 167 (1997) 470.
[18] L.P. Wang, W.T. Tysoe, Surf. Sci. 230 (1990) 74.
[19] G. Wu, B. Bartlett, W.T. Tysoe, Surf. Sci. (in press).
[20] L.P. Wang, R. Hinkelman, W.T. Tysoe, J. Electron Spectrosc. Relat. Phenom. 56 (1991) 341.
[21] H.M. Kennett, A.E. Lee, Surf. Sci. 48 (1975) 606.
[22] E.I. Ko, K.J. Madix, Surf. Sci. 109 (1981) 221.
[23] E. Bauer, H. Hoppa, Surf. Sci. 88 (1979) 31.
[24] C. Zhang, M.A. Van Hove, G.A. Somorjai, Surf. Sci. 149 (1985) 326.
[25] H.M. Kennett, A.E. Lee, Surf. Sci. 48 (1975) 624.
[26] J.W. Robinson (Ed.), Handbook of Spectroscopy, vol. 1, Chemical Rubber Co., Cleveland, OH, 1974.
[27] J.E. Deffeyes, A.H. Smith, P.C. Stair, Appl. Surf. Sci. 26 (1986) 517.
[28] J.L. Grant, T.B. Fryberger, P.C. Stair, Surf. Sci. 239 (1990) 127.
[29] M.K. Weldon, C.M. Friend, Surf. Sci. 321 (1994) L202.
[30] G. Wu, W.T. Tysoe, Surf. Sci. 383 (1997) 57.
[31] G.H. Smudde, Jr, M. Yu, P.C. Stair, J. Am. Chem. Soc. 115 (1993) 1988.
[32] N. Calderon, E.A. Ofstead, J.P. Ward, W.A. Judy, K.W. Scott, J. Am. Chem. Soc. 90 (1968) 4133.
[33] J.L. Wang, H.R. Menapace, J. Org. Chem. 33 (1968) 3794.
[34] D.T. Laverty, J.J. Rooney, A. Stewart, J. Catal. 45 (1976) 110.
[35] J.K. Kochi, Organometallic Mechanisms and Catalysis, Academic Press, New York, 1978.
[36] M. Ephritikhine, M.L.H. Green, J. Chem. Soc., Chem. Commun. (1976) 926.
[37] G.J.A. Adams, S.G. Davis, K.A. Ford, M. Ephritikhine, P.F. Todd, M.L.H. Green, J. Mol. Catal. 8 (1980) 15.
[38] J.C. Weast (Ed.), CRC Handbook of Physics and Chemistry, CRC Press, Cleveland, OH, 1968.
[39] R.W.G. Wykoff, Crystal Structures, vol. 1, Wiley, New York, 1963.